Available online at www.sciencedirect.com

ScienceDirect

Procedia Engineering 97 (2014) 1406 – 1415

Procedia Engineering

www.elsevier.com/locate/procedia

12th GLOBAL CONGRESS ON MANUFACTURING AND MANAGEMENT, GCMM 2014

Grey relational analysis based optimization of underwater Nd:YAG laser micro-channeling on PMMA

Bappa Acherjee[a,*], Shashi Prakash[b], Arunanshu S. Kuar[c], Souren Mitra[c]

[a] *Production Engineering Department, Birla Institute of Technology: Mesra, Deoghar Campus, Deoghar - 814142, India*
[b] *Mechanical Engineering Department, Indian Institute of Technology Patna, Patna – 800013, India*
[c] *Production Engineering Department, Jadavpur University, Kolkata - 700032, India*

Abstract

Laser based micro-channeling is emerging as the most widely used process for fabrication of polymer based micro-fluidic devices. Nd:YAG lasers are one of the most favoured laser system by industries involved in laser based material processing. However, they have not been fully explored for micro-level processing. In this research work, Nd:YAG laser has been utilized in fabrication of micro-channels on PMMA in underwater condition. The input parameters have been chosen as lamp current, scanning speed, pulse frequency and pulse width. Depth, burr height and burr width of the micro-channel have been taken as output quality characteristics. Taguchi methodology in combination with grey relational analysis has been employed to determine the optimal parametric condition for satisfying multiple objectives at same time. Underwater laser processing has resulted in minimization of undesirable effects of laser processing like heat affected zone and redeposition around the micro-channels resulting in cleaner and finer structure than open air processing.

Selection and peer-review under responsibility of the Organizing Committee of GCMM 2014

Keywords: underwater laser machining; micro-channels; grey relational analysis

1. Introduction

Laser based micro-fabrication processes are always subjected to heat based undesirable effects, especially when machining with infra-red lasers (1μm wavelength). On the other hand these lasers are robust in structure and easy to maintain in industries. Lasers with nano-second pulse duration results in thermal damages around the micro-structure while patterning the polymer based micro-fluidic devices. For fabricating the micro-fluidic devices of high qualities,

* Corresponding author. Tel.: +91-6432-292565; fax: +91-6432-292565.
E-mail address: a.bappa@yahoo.com; bappa.rana@gmail.com

Selection and peer-review under responsibility of the Organizing Committee of GCMM 2014
doi:10.1016/j.proeng.2014.12.422

Nomenclature

A	Ampere
Hz	Hertz
F	pulse frequency
P	lamp current
S	cutting speed
W	pulse width
m	number of quality characteristics
x	normalized results
x^0	ideal normalized result
y	quality characterstic
w	weighting factor
γ_m	total mean of the grey relational grades
γ_{opt}	optimum grey relational grade
ζ	distinguishing coefficient
ξ	grey relational coefficient
μm	micro meter

it is very essential to reduce and minimize those undesirable effects. Underwater laser processing was first utilized by Ageev (1975) to study material ablation during emission spectroscopy. Underwater laser processing is a novel technique to produce clean, clog free micro-features on materials by utilizing local cooling effect as well as reducing the redeposition of ablated material on the surface. The material ablation phenomenon in underwater condition is entirely different from open air condition. During underwater ablation, the optical breakdown of molecules and limited expansion of plasmas take place (Wang et al., 2006). Due to limited expansion of laser formed plasma, the recoil pressure, generated due to plasma shock waves, increases manifold (Chen et al., 2004; Li et al., 2005). This form of ablation increases the part of cold ablation in contrast to only thermal ablation in open air condition. This also results in increase of material ablation rate in underwater condition. The redepository materials are generally lighter than water and do not get redeposit on the work-piece surface instead flows in the water. However, it is not always the case, especially in continuous wave lasers having pulse width durations more than 100μs (Morita et al., 1988). Choo et al., (2004) performed the micro-machining on silicon in both open air and underwater condition using excimer lasers. A significant amount of thermal damage has been observed in open air processing, while the underwater processing has resulted in absence of thermal damage. Underwater laser processing has also been proved to be very beneficial in through cutting. Muhammad et al., (2010) performed the cutting operation in fibre laser cutting of 316L stainless steel tubes of 200 μm thickness and 4mm diameter. The underwater cutting results in zero back wall damage. Dross and heat affected zone has also been minimized.

Micro-channel based micro-fluidic devices have diversified application in different areas. While metallic and semiconductor based micro-channels are mainly used for cooling purpose in electronic devices, the polymer based micro-fluidic devices are generally used for bio-analytical devices like electrophoresis, DNA analysis and blood protein analysis. Polymers have slowly replaced the glass based micro-fluidic devices. Fabricating micro-channels on glass is time consuming, as well as, clean room facilities are needed. PMMA (Poly-methyl-meth-acrylate) has been proved to be most economical replacement of glass based devices (Chantal and Khan, 2006). However, most of the polymers are more susceptible to heat and therefore clean laser processing of such polymers is always a challenge. The laser processing of polymers has been studied by Chang and Molian (1999) under ethanol and methyl alcohol using excimer laser of 193 nm. They investigated the chemical assisted laser based ablation on different polymeric materials like PMMA, polyethylene and polypropylene. They concluded that material removal in polyethylene and polypropylene takes place layer by layer in order to maintain the homogeneity, however, the PMMA etches faster in presence of ethyl alcohol and methanol when compared to air. The underwater processing on silicon wafers has been conducted by wee et al., (2011). The micro-drilling operation has been performed on silicon in open air as well as in flowing water condition. The underwater drilling resulted in lesser thermal damage and heat affected zone on both top side as well as bottom side while maintaining the straightness of the hole. On the other hand the underwater operation has also resulted in increased material removal rate. So, it can be concluded that most

of the studies in underwater conditions have been made on lasers having short wavelength lasers (UV lasers). However, the longer wavelength lasers where material removal takes place more due to thermal ablation have not been studied comprehensively.

In this research work, fabricating micro-channels based on underwater laser processing has been investigated. Nd:YAG laser is used to produce micro-channels on PMMA. Underwater laser processing has been fundamentally utilized for reducing the undesirable effects of laser based micro-processing. The experiments have been designed based on L-16 orthogonal array using Taguchi methodology. Grey relational analysis in combination with Taguchi method is used to find the optimum process parameters to fulfil multiple objectives, simultaneously.

2. Experimental work

An L-16 orthogonal array has been used to design the experimental matrix. Thus total 16 experiments have been performed in order to study the laser micro-channeling on PMMA. A computer numerical controlled Nd:YAG laser (make: M/s Sahajanand Laser Technology, India) has been used in this research work. This is a pulsed laser system, having one cycle time of approximately 120 ns. The laser beam comes out of main lasing unit has 125 μm diameter and M^2 value of the beam is 1.15. Four key process parameters, which affect the process significantly, have been taken as input factors namely, lamp current, P, pulse frequency, F, pulse width, W, and cutting speed, S. Lamp current directly corresponds to total laser fluence or energy consumed by laser to emit desired pulses. Pulse frequency is the number of pulses emitted by laser per unit time. Pulse width denotes the percentage of "ON" time duration per cycle time. Cutting speed represents the speed of movement of laser head with respect to the workpiece or vice-versa. Four levels of each factors has been identified based on the pilot experiments. Table 1 shows the values of different input process parameters at different levels. The heat affected zone (HAZ) has been found to be surrounded by burrs and irregular protrusions of very small sizes. Hence heat affected zone has been categorised into two output parameters, burr width and burr height. The width of burrs has been considered to be equal to width

Table 1. Laser micro-channeling process parameters and their levels

Character	Parameter	Level			
		1	2	3	4
P	lamp current (A)	14	15	16	17
F	pulse frequency (kHz)	2	3	4	5
W	pulse width (%)	6	9	12	15
S	cutting speed (mm/s)	0.2	0.3	0.4	0.5

Table 2 Experimental lay out and multi-performance results

Experiment	Process parameters				Channel depth	Burr height	Burr width
no.	P (A)	F (kHz)	W (%)	S (mm/s)	(μm)	(μm)	(μm)
1	1	1	1	1	66.37	22.44	59.96
2	1	2	2	2	41.21	11.79	54.87
3	1	3	3	3	92.85	29.52	65.11
4	1	4	4	4	87.26	9.65	90.68
5	2	1	2	3	83.62	20.66	71.16
6	2	2	1	4	80.03	33.19	87.13
7	2	3	4	1	95.36	5.89	33.05
8	2	4	3	2	113.6	13.90	60.56
9	3	1	3	4	32.43	10.21	128.15
10	3	2	4	3	51.35	11.18	81.65
11	3	3	1	2	106.32	48.02	73.67
12	3	4	2	1	97.82	32.12	94.17
13	4	1	4	2	107.95	29.52	72.96
14	4	2	3	1	88.90	38.44	67.97
15	4	3	2	4	111.50	79.52	105.95
16	4	4	1	3	121.63	99.72	95.56

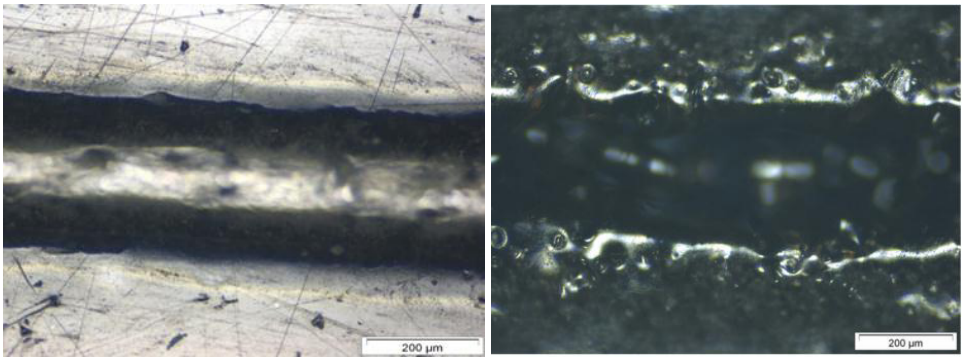

Fig. 1. Photographic view of micro-channel fabricated on PMMA using Nd:YAG pulsed laser (a) in underwater condition, and (b) in open air condition

of HAZ. Hence these three parameters have been taken as output parameters: (a) micro-channel depth, (b) burr width, and (c) burr height. The output parameters have been measured by using Olympus-STM-6, a 3-dimensional optical measuring microscope. For reducing the errors during measurement, each response has been measured at three different locations across the channel and their statistical average has been used. Distilled water at room temperature (24-25^0 C) has been used as water medium because of easy availability and its non-reactive nature to work-piece material even at higher temperatures. For each experiment fresh water has been used. To maintain the height of the water level fixed at 1 mm, volume method has been utilized. In this method the height has been measured using vernier height gauge connected to electronic circuit. As soon as the tip of the vernier gauge comes in contact with water, the electricity flows thus completing the circuit. By using this method on trial and error basis, the corresponding volume subjected to 1mm above the work-piece has been determined and used in all the experiments. The same level of water level has been reported by Muhammad and Li, 2012. The experimental layout for the machining parameters using the L16 orthogonal array and the experimental results are presented in Table 2. Fig. 1 shows the micro-channels fabricated on PMMA using Nd:YAG pulsed laser (a) in underwater condition, and (b) in open air condition.

3. Results and discussion

The parameter design of Taguchi method utilizes orthogonal arrays to minimize the time and cost of experiments in analyzing all the factors and to find the optimal parameter combination. In this process the response values are transformed into signal-to-noise (S/N) ratios. Here, the ‘signal’ represents the desirable value and the ‘noise’ represents the undesirable value and S/N ratio expresses the scatter around the desired value. S/N ratio for each level of process parameters is computed based on the S/N analysis which can be utilised to study the effect of machining parameters on micro-channel quality characteristics. Fig. 2 shows the main effect plot of S/N ratios of channel depth. From the figure it can be observed that the depth of the micro-channel shows a linear increase and decrease behaviour with lamp current. This is due to combined effect of transferring more power and increased rate of heat transfer in the underwater machining. As the lamp current increases the photon energy and corresponding beam energy also increases. However, the higher energy photons cause more amount of plasma to be generated and the plasma prevents the laser beams with moderate energy to strike the inner surface of the micro-channel. However, as the beam power is further increased beyond a threshold, the laser beams become able to penetrate through plasma, therefore resulting in increase in depth. Also when the pulse frequency increases, the number of pulses on particular area also increases but the energy content of each pulse decreases. However, larger number of pulses produces more charring and burning effect on the edges and helps in penetrating through limited plasma zone as well as increase in recoil pressure therefore increasing the depth of the micro-channel. Increasing the pulse width determines the percentage of ON time therefore pulse interaction time to be more. However, more energy transfer to the surface also creates a plasma zone inside the channel which further prevents the penetration of laser beam inside the material. However, as the beam width crosses certain threshold, the beam energy becomes sufficient to penetrate through the plasma and results in increase in depth. The effect of cutting speed can be explained as the speed

decreases the depth increases since the beam strikes for longer duration. At the same time when speed is reduced continuously, the local cooling takes place more effectively and depth of the channel decreases.

Fig. 3 shows the S/N ratio plot for Burr height. Burrs are found to be formed over the entire heat affect zone. While some burrs are formed due to redepository material, some gets generated as protruded surface due to uneven heat generation on the surface. The burr height decreases with increase in lamp current. The burrs are formed mainly due to heat distribution at the surface rather than at the base of formed depth. Burr height initially decreases with increase in pulse frequency but later increases as the frequency increases. This is due to the reason, that more number of pulses create more charring and burning effect on the edges which results in heat based damage on the surface rather than inside the depth. As the pulse width increases, the time duration of energy transfer also increases which further increases the heat affected zone and results in uneven heat distribution on the surface. Therefore it results in increase of burr height. As the speed increases, the amount of energy transfer decreases and therefore the burr formation also decreases. However, at higher speeds the energy transfer is more visible at surface and therefore, burr formation takes place and results in increase in burr height.

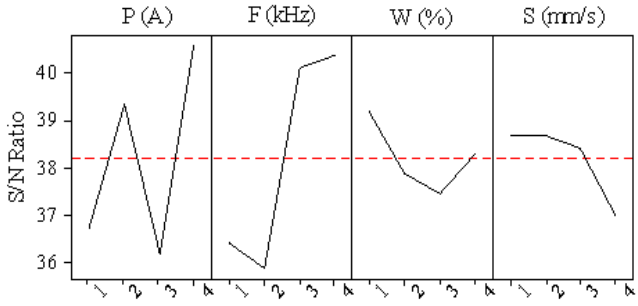

Fig. 2. S/N ratio plot of channel depths

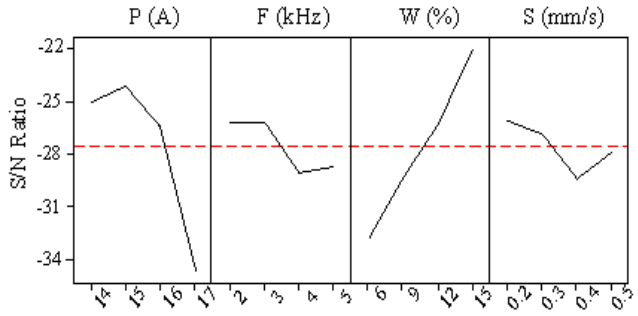

Fig. 3. S/N ratio plot of burr heights

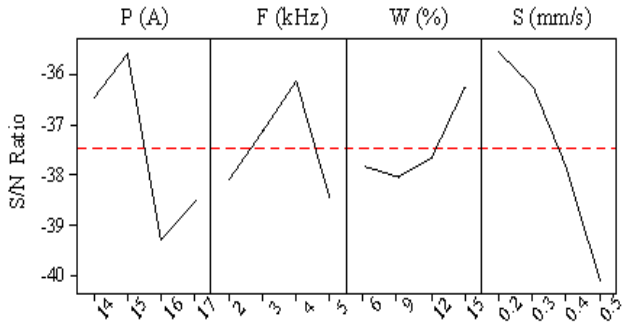

Fig. 4. S/N ratio plot of burr width

The burr width directly indicates the extent of heat affected zone. Fig. 4 shows the S/N ratio plot for Burr width. Burr width initially increases with lamp current and then decreases. However at higher current levels the width starts increasing. Higher lamp current also increases the rate of energy transfer and does not contribute to surface effects. However, if the whole surface temperature crosses certain temperature threshold, usually equal to glass transition temperature, the heat affected zone starts to begin. As the pulse frequency increases the average pulse energy starts to decrease and therefore more surface effects begin to appear however beyond a certain frequency threshold, the energy of the pulses become so much low to induce heat affected zone. Increasing the pulse width directly results in more energy transfer to the surface and therefore results in increase of burr width. Increase the speed directly causes the lesser material deposition per unit area and therefore results in lower burr width.

3.1. Multi-objective optimization using grey relational analysis:

It is always necessary to find favourable process conditions capable of producing desired micro-channel quality, defined in terms of desired quality characteristics. However, this optimization should be performed in such a way that all the objectives are fulfilled simultaneously. Optimization of multiple quality characteristics is much more complicated than that of a single quality characteristic. Improving one particular quality characteristic would possibly lead to serious degradation of the other critical quality characteristics. Grey based Taguchi method is proven to be useful for tackling such optimization problems (Kuar et al., 2012). In this method, the original data is normalized in order to make it of one dimension or dimensionless. A grey relational coefficient represents the relationship between original data and normalized data. A grey relational grade is obtained by weighted averaging the grey relational coefficients of each output parameter. This grey relational grade is used in performing the multi-objective optimization. The input parameter values associated with highest grey relational grade represents the most optimized value for desired results (Acherjee et al., 2011).

In grey relational analysis, each output parameter is normalized in the range of 0 to 1 to obtain a comparable sequence by making magnitude of the original data of order one and dimensionless. Burr width and burr height have lower-the-better quality characteristics. For lower-the-better quality characteristic, the normalized results, x_{ij}, can be expressed as:

$$x_{ij} = \frac{\max_j y_{ij} - y_{ij}}{\max_j y_{ij} - \min_j y_{ij}} \tag{1}$$

Micro-channel depth has higher-the-better (HB) quality characteristics. The normalized results, x_{ij}, for higher-the-better quality characteristic can be expressed as:

$$x_{ij} = \frac{y_{ij} - \min_j y_{ij}}{\max_j y_{ij} - \min_j y_{ij}} \tag{2}$$

where y_{ij} is the ith quality characteristic in the jth experiment. Larger normalized results correspond to the better quality and the best-normalized result should be equal to 1. The output data for channel depth, burr height and burr width, obtained after normalization has been shown in Table 3.

Grey relational coefficients are calculated to express the relationship between the ideal and the actual experimental results. The grey relational coefficient, ξ_{ij}, can be expressed as:

$$\xi_{ij} = \frac{\min_i \min_j |x_i^0 - x_{ij}| + \zeta \max_i \max_j |x_i^0 - x_{ij}|}{|x_i^0 - x_{ij}| + \zeta \max_i \max_j |x_i^0 - x_{ij}|} \tag{3}$$

where x_i^0 is the ideal normalized result (i.e., best normalized result = 1) for the ith quality characteristics and $\zeta \in [0,1]$ is a distinguishing coefficient. Here the value of ζ is set to be 0.5, the quantity used in most situations. The grey relational coefficient obtained for the each experimental run of L-16 orthogonal array is shown in Table 4.

After obtaining the grey relational coefficients, a weighting method is used to integrate the grey relational coefficients of each experiment into the grey relational grade. The overall evaluation of the multiple quality characteristics is based on the grey relational grade, which is given by:

$$\gamma_j = \frac{1}{m}\sum_{i=1}^{m} w_i \xi_{ij} \tag{4}$$

where γ_j is the grey relational grade for the jth experiment, w_i is the weighting factor for the ith quality characteristic and m is the number of quality characteristics. In calculating the grey relational grades the weighting ratio for micro-channel depth, burr width and burr height are set as 2:1:1, respectively. The experiment corresponding to highest value of grey relational grade is considered to be the closest to the optimal value of the desired multiple responses. Table 7 shows grey relational grade for each experiment. Thus experiment no. 7 corresponds to highest grey relational grade among 16 experiments, and is supposed to be the closest to the desired characteristics.

Table 3. Data preprocessing of the experimental results

Experiment no.	Grey relational generating		
	Channel depth	Burr height	Burr width
Ideal sequence	1	1	1
1	0.380	0.824	0.717
2	0.098	0.937	0.771
3	0.677	0.748	0.663
4	0.615	0.960	0.394
5	0.574	0.843	0.599
6	0.534	0.709	0.431
7	0.705	1.000	1.000
8	0.910	0.915	0.711
9	0.000	0.954	0.000
10	0.212	0.944	0.489
11	0.828	0.551	0.573
12	0.733	0.720	0.357
13	0.847	0.748	0.580
14	0.633	0.653	0.633
15	0.886	0.215	0.233
16	1.000	0.000	0.343

Table 4. The calculated grey relational coefficients

Experiment no.	Grey relational coefficient		
	Channel depth	Burr height	Burr width
1	0.4466	0.7392	0.6386
2	0.3567	0.8883	0.6855
3	0.6078	0.6650	0.5973
4	0.5648	0.9258	0.4521
5	0.5399	0.7606	0.5551
6	0.5174	0.6321	0.4679
7	0.6293	1.0000	1.0000
8	0.8474	0.8542	0.6335
9	0.3333	0.9157	0.3333
10	0.3882	0.8987	0.4945
11	0.7445	0.5269	0.5393
12	0.6520	0.6414	0.4376
13	0.7653	0.6650	0.5437
14	0.5767	0.5904	0.5766
15	0.8149	0.3892	0.3948
16	1.0000	0.3333	0.4320

The application of this optimization technique converts the multiple quality characteristics to a single performance characteristic i.e., grey relational grade and, therefore, simplifies the optimization procedure. Optimal micro-channelling parameters are then determined by the Taguchi method using grey relational grade as the single quality

index (output). Fig. 5 shows the S/N ratio plot of grey relational grades. The best values of micro-channelling process parameters, for maximizing the grey relational grade, are identified from the S/N ratio plot of grey relational grades. Based on this graph, the optimal parameter setting is to maintain lamp current at level 2 (P = 15 A), pulse frequency at level 4 (F = 5 kHz), pulse width at level 4 (W = 15 %) and cutting speed at level 2 (S = 0.3 mm/s) for maximizing the channel depth and minimizing the burr height and burr depth, simultaneously. The predicted value of gray relational grade at optimal parameter setting is found to be greater than that obtained in experiment no. 7.

Table 5. Grey relational grades and its order

Experiment no.	Grey relational grade	Order
1	0.5678	13
2	0.5718	12
3	0.6195	7
4	0.6269	6
5	0.5989	9
6	0.5337	15
7	0.8147	1
8	0.7956	2
9	0.4789	16
10	0.5424	14
11	0.6388	5
12	0.5957	10
13	0.6848	4
14	0.5801	11
15	0.6034	8
16	0.6913	3

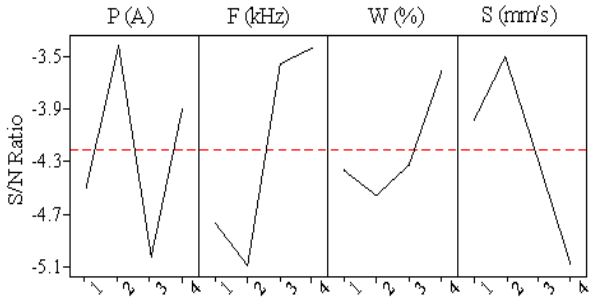

Fig. 5. S/N ratio plot of means of grey relational grades

The results of ANOVA test for grey relational grades are given in Table 6. While considering the overall feature of the micro-channel, it is found that pulse repetition frequency is the most predominant factor followed by lamp current, cutting speed and pulse width.

Table 6. Results of the ANOVA for grey relational grades

Source	Degrees of freedom	Sum of squares	Mean squares	F-value	Prob>F
P	3	0.0336	0.0112	13.47	0.030
F	3	0.0443	0.0148	17.74	0.021
W	3	0.0125	0.0042	5.01	0.109
S	3	0.0269	0.0090	10.77	0.041
Error	3	0.0025	0.0008		
Total	15	0.1197			

3.2. Confirmation experiments:

In order to verify the predicted values at optimum condition, confirmation experiments have been performed. The optimum grey relational grade, γ_{opt}, is calculated as:

$$\gamma_{opt} = \gamma_m + \sum_{i=1}^{q} (\bar{\gamma}_i - \gamma_m) \tag{5}$$

where, γ_m is the total mean of the grey relational grade, $\bar{\gamma}_i$ is the mean grey relational grade of *i*th parameter at the optimal level, and q is the number of machining parameters that significantly influence the quality characteristics. Confirmation test has been conducted with optimal setting and has been presented in Table 7. The grey relational grade has been improved by 0.1577, when compared with an initial parameter setting. As shown in Table 7, at optimal parameter setting, the channel depth is increased from 107.95µm to 114.57µm, burr height is minimized from 29.52 µm to 8.23µm and burr width is minimized from 72.96 to 54.33.

Table 7 Result of confirmation experiment

	Initial parameter setting	Optimal parameters	
		Prediction	Experiment
Level	$P_4F_1W_4S_2$	$P_2F_4W_4S_2$	$P_2F_4W_4S_2$
Channel depth (µm)	107.95		114.57
Burr height (µm)	29.52		8.23
Burr width (µm)	72.96		54.33
Grey relational grade	0.6848	0.8384	0.8425
Improvement of the grey relational grade = 0.1577			

4. Conclusion

Underwater laser micro-channeling has been proved to be very effective in creating clean, burr-free structures and can be readily used in micro-fluidic based devices. The presence of water not only reduces the heat affected zone but also helps in preventing redepository material on the work-piece surface. The structure has been found to be clear and free from debris. The edges of the micro-channels were found to be straight and parallel, therefore making the process of underwater micro-channeling more preferable than in open air.

Grey relational analysis has been found to be an effective yet simple method for optimizing multi-characteristic process. Experiments have been designed according to L-16 orthogonal array. The significance of the process parameters on overall micro-channel quality is evaluated quantitatively by analysis of variance technique. The results of ANOVA reveal that the overall feature of the micro-channel is affected predominantly by pulse repetition rate. The confirmation test verifies that the quality characteristics of laser micro-channeling process, such as micro-channel depth, burr width and burr height, can be improved simultaneously by the method proposed in this study.

References

[1] Acherjee, B., Kuar, A.S., Mitra, S., Misra, D., 2011, Application of grey-based Taguchi method for simultaneous optimization of multiple quality characteristics in laser transmission welding process of thermoplastics, International Journal of Advanced Manufacturing Technology 56, 995-1006.

[2] Ageev, VA., 1975, Investigation of optical erosion of metals in liquids, Joural of Applied Sprectoscopy 23(1), 903-906.

Chang, T.C., Molian, P.A., 1999, Excimer pulsed laser ablation of polymers in air and liquids for micromachining applications, Journal of Manufacturing Processes 18 (2), 1-17.

[3] Chantal, G., Khan, M., 2006, Laser processing for bio-microfluidic applications (part II), Analytical and Bioanalytical Chemistry 385, 1362-1369.

[4] Chen, X., Xu, R.Q., Chen, J.P., Lu, J., Ni, X.W., 2004, Shock-wave propagation and cavitation bubble oscillation by Nd:YAG laser ablation of a metal in water, Applied Optics 43 (16), 3251–3257.

[5] Choo, K.L., Ogawa, Y., Kanbargi, G., Otra, V., Raff, L.M., Komanduri, R., 2004, Micromachining of silicon by short-pulse laser ablation in air and under water, Materials Science and Engineering A 372, 145–162.

[6] Kuar A.S., Acherjee, B., Ganguly, D., Mitra, S., 2012, Optimization of Nd:YAG laser parameters for microdrilling of alumina with multiquality characteristics via grey–Taguchi method, Materials and Manufacturing Processes 27, 329–336.

[7] Li, M., Zhang, H., Shen, Z., Lu, J., Ni, X., 2005, Physical analyses of optical breakdown and plasma formation in water induced by laser, Acta Photonica Sinica 34 (11), 1610–1614.

[8] Morita, N., Ishida, S., Fujimori, Y., Ishikawa, K., 1988, Pulsed laser processing of ceramics in water, Applied Physics Letters 52(23), 1965–1966.
[9] Muhammad, N., Li, L., 2012, Underwater femtosecond laser micromachining of thin nitinol tubes for medical coronary stent manufacture, ApplPhys A 107, 849-861.
[10] Muhammad N, Whitehead D, Boor A, Li L, 2010, Comparison of dry and wet fibre laser profile cutting of thin 316L stainless steel tubes for medical device applications, Journal of Materials Processing Technology 210, 2261–2267.
[11] Wang, S.C., Lee, C.Y., Chen, H.P., 2006, Thermoplastic microchannel fabrication using carbon dioxide laser ablation, Journal of Chromatography A 1111 (2), 252 – 257.
[12] Wee, L.M., Ng, E.Y.K., Prathama, A.H., Zheng, H., 2011, Micro-machining of silicon wafer in air and under water, Optics & Laser Technology 43, 62–71.